

NASA Contractor Report 204137  
ICOMP-97-06; CMOTT-97-01  
AIAA-97-3243

1N-34  
067134

# Application of Low Dimensional Manifolds in NO<sub>x</sub> Prediction

A.T. Norris

*Institute for Computational Mechanics in Propulsion  
and the Center for Modeling of Turbulence and Transition  
Cleveland, Ohio*

August 1997

Prepared for  
Lewis Research Center  
Under Cooperative Agreement NCC3-534



National Aeronautics and  
Space Administration





# APPLICATION OF LOW DIMENSIONAL MANIFOLDS IN NO<sub>x</sub> PREDICTION

A. T. Norris \*

Institute for Computational Mechanics in Propulsion  
and the Center for Modeling of Turbulence and Transition  
NASA Lewis Research Center, Cleveland Ohio.

## **Abstract**

A new post-processing technique has been developed, based on the Intrinsic Low Dimensional Manifold (ILDM) method of Maas and Pope<sup>1,2</sup>.

The ILDM method is a dynamical systems approach to the simplification of large chemical kinetic mechanisms. By identifying low-dimensional attracting manifolds, the method allows complex full mechanisms to be parameterized by just a few variables: In effect, generating reduced chemical mechanisms by an automatic procedure. These resulting mechanisms however, still retain all the species used in the full mechanism.

The NO<sub>x</sub> post-processor takes an ILDM reduced mechanism and attempts to map this mechanism to the results of a CFD calculation. This mapping allows the NO<sub>x</sub> concentrations at each grid node to be obtained from the ILDM reduced mechanism, as well as other trace species of interest. Because a mapping procedure is used, this method is very fast, being able to process one million node calculations in just a few minutes.

## **Introduction**

The ability to predict NO<sub>x</sub> in CFD calculations of reacting flows is constrained by the trade-off between accuracy and available computing resources.

---

\* Senior Research Associate, Member AIAA  
Copyright ©1997 by the American Institute of Aeronautics and Astronautics, Inc. No copyright is asserted in the United States under Title 17, U.S. Code. The U.S. Government has a royalty-free licence to exercise all rights under the copyright claimed herein for Governmental Purposes. All other rights are reserved by the copyright owner.

For fluid design calculations, it is enough to get the values of density and temperature correct, and so fairly simple chemical mechanisms may be employed, with good results.

However the prediction of trace species, such as NO, requires the use of a significantly more complex kinetics scheme, with the resulting increase in computational effort required to solve the problem. For example, a simple two-step mechanism will have six species (Fuel, H<sub>2</sub>O, CO, CO<sub>2</sub>, O<sub>2</sub>, N<sub>2</sub>) and two rate equations. To predict NO by the Zeldovich mechanism will require adding 5 more species (OH, O, H, N, NO) and six more rate equations. Clearly this has more than doubled the complexity of the problem and the CPU time required.

To overcome this increase in complexity, post-processing is an attractive option, with the promise of quickly obtaining the NO<sub>x</sub> fields when the solution of the major species and velocity fields has converged. To do this, two main approaches are employed.

In the first, the composition and temperature at each node are used to obtain the equilibrium value of NO<sub>x</sub>. This has the advantage of being very quick, but will naturally over-predict the value of NO<sub>x</sub> at each point. Due to the very slow rate of NO<sub>x</sub> formation under most conditions, it may significantly over-predict the value. The advantage of this method is its speed, and that it does not need to know anything about the composition at neighbouring nodes.

The second technique employed is an iterative, frozen-composition method. In this the values of velocity, density and major species compositions are frozen and the species transport equations are

solved for the minor species. The disadvantage of this technique is the time required to perform the iterations to convergence. Typically this can be of a similar CPU time as the original calculation. In addition, the technique is not code independent. i.e. The CFD results from an unstructured code will have to be processed differently than those from a structured code. The advantage is that the NOx reaction rates are not assumed to be fast, and so finite rate effects are accounted for.

In this paper, an approach is outlined that attempts to provide the equilibrium approach with the finite rate effects available to the iterative scheme.

To achieve this, an Intrinsic Low Dimensional Manifold (ILDM) simplification of a full mechanism is performed, so that all species are represented as functions of a mixture fraction  $\xi_I$  and a progress variable  $Y_{p_I}$ . Then for each node in the CFD data, a mixture fraction  $\xi_C$  and progress variable  $Y_{p_C}$  is obtained and by mapping the ILDM variable onto the CFD values, a value for the trace species may be obtained.

## ILDM Method

The ILDM method employed in this work is that used in the NASA Lewis ILDM code.<sup>3</sup> In this code, the ILDM simplified mechanism is obtained by a trajectory-generated technique, described by Pope and Maas<sup>4</sup>. In this method, the full mechanism is parameterized by two scalars, a mixture fraction based on atom concentrations and a progress variable, based on either species mass fractions, temperature or Gibbs function. The resulting species concentrations, rates and properties are stored in look-up tables. A more detailed description can be obtained by Norris<sup>3</sup>.

One concern in the creation of the ILDM tables is that because the reaction rate of NOx is very slow, the ability to interpolate accurately may be compromised near the fully burnt limit of  $Y_{p_I}$ . This is because the progress variable will only change a small amount, while the NOx values can change by an order of magnitude. To counter this, the look-up table has been modified to cluster the nodes near the fully burnt value. In addition, the choice of temperature as the progress variable is found to give the best resolution for NOx values.

## Post-Processor

The post-processor performs the functions of reading in the CFD data, obtaining the values of  $\xi_C$  and  $Y_{p_C}$ , and then mapping the composition at each node to the manifold.

The mixture fraction of the CFD data can be obtained by several methods, each based on atom population. The mixture fraction based on the  $m$  atom,  $\xi_m$  is given by

$$\xi_m = \frac{Y_m - Y_{m,air}}{Y_{m,fuel} - Y_{m,air}} \quad (1)$$

where  $Y_m$  is the mass fraction of the  $m$  atom,  $Y_{m,fuel}$  is the mass fraction of the  $m$  atom in the fuel stream and  $Y_{m,air}$  is the mass fraction of the  $m$  atom in the air stream.

The three options for progress variable are species, temperature or Gibbs function based. The species option allows one to obtain the progress variable as a normalized mass fraction of a chemical species, or the sum of several chemical species. For example one could chose a mixture fraction based on the mass fraction of CO<sub>2</sub>, or the sum of the mass fractions of CO<sub>2</sub> and H<sub>2</sub>O. The only restriction on this choice is that the resulting quantity should be single-valued. For this reason, a progress variable based on the mass fraction of OH would not be acceptable, as the OH value rises, peaks and then drops down to an equilibrium value. Another option is to use temperature as a progress variable, while the Gibbs function provides the third option. In all of these three cases, the progress variable must be the same as the one used to obtain the ILDM table.

Having obtained  $\xi_C$  and  $Y_{p_C}$  for each CFD data point, the NOx value is simply obtained by interpolating from the ILDM table at the equivalent  $\xi_I$  and  $Y_{p_I}$  locations.

## Test Cases

Three test cases were employed to evaluate the performance of the post-processor: A hydrogen-air can combustor, a methane-air combustor and a jet-a-air problem.

The hydrogen-air combustor consists of a stepped tube, with swirling air being injected in radially. Hydrogen fuel is injected in downstream of the air inlet, without swirl. Initial conditions for this case

are air at 804K, hydrogen at 305K and a pressure of 20 atm. In addition, several other inlet conditions were investigated, corresponding to different operation conditions.

Due to the sensitive nature of the methane and JetA cases, the configuration of these problems will not be reported. However the initial conditions for the methane case are a fuel inlet temperature of 305K, an air temperature of 950K and a pressure of 20 atm. The JetA case has initial air temperatures of 740K, with a fuel temperature of 350K and a pressure of 10 atm.

Data available for these flows consists of experimental measurements of NOx levels at the exit plane of the hydrogen-air cases, while the methane and JetA configurations have the values of NOx obtained at each data point by the inclusion of the Zeldovich mechanism in their reduced mechanism. It should be noted that the CFD results for all but the first hydrogen-air setup were not run to a fully converged condition. However the results are included for completeness.

The full mechanisms used to obtain the ILDM tables are the hydrogen-air mechanism of Miller and Bowman <sup>5</sup>, the methane-air mechanism of Miller and Bowman <sup>5</sup> and the JetA-air mechanism of Kollrack <sup>6</sup>.

## Results

To address the accuracy of the mapping procedure, the scalar fields for known major species were extracted by the postprocessor and compared to the CFD results. The mixture fraction was obtained based on the mass fraction of the H atom for the H<sub>2</sub>-air case, and the C atom for the methane and jetA cases. In all cases, the temperature was used as the progress variable.

For the hydrogen-air Case 1, the predicted mass fraction of H<sub>2</sub>O is plotted against the CFD results in Fig 1. As can be seen, there is a good agreement between the CFD result and the manifold prediction. For the methane case, the predicted mass fractions of CO<sub>2</sub> and H<sub>2</sub>O are compared to the CFD results in Fig 2. and 3. respectively. Again there is very good agreement, except for the very low values. It can be seen that the values of CO<sub>2</sub> are underpredicted while the mass fractions of H<sub>2</sub>O are overpredicted. For the JetA example, the predicted mass fractions of CO<sub>2</sub> and H<sub>2</sub>O are compared to the CFD results in Fig 4. and 5. respectively. In

this case, the values of CO<sub>2</sub> are underpredicted for the entire range of values, while the H<sub>2</sub>O values are overpredicted. This deviation in the results will be discussed in the next section.

For the hydrogen-air cases, the NO exit concentration was predicted and compared to experimental data. The results of this are shown in Table 1. It can be seen that a reasonable agreement is obtained in all 5 cases. It should be noted that the first case is the only one to have converged fully, thus the results for the other four may be somewhat suspect. For the hydrogen case, no CFD values of NOx were available.

Hydrogen-Air NO Prediction Performance.

Case Number	Prediction	Experiment
Case 1	20.5 ppm	21.6-26.5 ppm
Case 2	6.9 ppm	10.6 ppm
Case 3	4.9 ppm	12.0 ppm
Case 4	13.9 ppm	3.1 ppm
Case 5	28.5 ppm	35.1 ppm

For the methane and JetA case, there are no experimental results available, and so the NOx predicted by the post-processor was compared to the CFD values.

In the Methane case, a reasonable agreement was obtained between the the prediction and the CFD results. A small percentage of results were underpredicted, and can be seen as the band of points lying to the left of the diagonal line in Fig 6.

For the JetA case shown in Fig. 7, the predicted NOx does not agree well with the CFD data, except at the high concentration levels.

## Discussion

The results described in the previous section will now be discussed.

For the hydrogen-air case, a very good agreement was obtained between the predicted H<sub>2</sub>O values and the CFD results. In addition, the predicted values at the combustor exit plane showed very good agreement with the experimental value. The cost of doing the ILDM prediction was only a few minutes to generate the look-up table and a negligible amount of CPU time to perform the interpolation. For this case then, the procedure looks very promising.

For the Methane case, the CO<sub>2</sub> and H<sub>2</sub>O results were very good, except at low concentrations. This

is caused by a combination of two factors. Firstly, the low concentration values correspond to very lean or unburnt compositions. Under these conditions, it is likely that mixing is a more important process than reaction, and so the ILDM table will not represent the state of the composition well. It is possible to include mixing in the table generation process, which may help this problem, but it has not been done in this case. The second factor is that the reduced mechanism may not agree with the ILDM scheme in certain regions. This would result in the compositions at the same progress variable differing between the two methods, and so the mapping not agreeing.

The comparison of the NO values for the methane case does not exhibit the nice one-to-one agreement of the major species. However it should be considered that the majority of data points do agree within an order of magnitude at the worst, and the high concentration values by a factor of 2. In addition, the values obtained by the CFD results can by no means be considered a true solution.

For the JetA case, there is not a very good agreement between the predicted and the CFD results for the major species. In this case, it is probably the full mechanism from which the ILDM table was obtained that is at fault. This mechanism is very old, and contains many outdated values for the individual rate expressions. In addition, the values of NO are only obtained by a Zeldovich mechanism, rather than the more complete mechanisms used in the hydrogen and methane cases. Despite the bad agreement though, the predicted NO values did show the right trend.

Because of the non-iterative nature of this post-processing technique, the transport, (or advection) of NO<sub>x</sub> is not accounted for explicitly. To illustrate this point, consider a 1D combustion problem. Initially, the fuel and air have mixed and start to react. Moving downstream the composition approaches the fully burnt state, and after sufficient time reaches it. In this example, the NO<sub>x</sub> post-processor would show the correct rise in NO<sub>x</sub> level, until the fully burnt state was reached. After the fully burnt state was reached, the post processor would predict a constant NO<sub>x</sub> concentration. However in reality, the NO<sub>x</sub> levels would continue to climb because the time scales of the NO<sub>x</sub> production are much slower than those of the major reaction components. The conclusion to be drawn from this is that this method will work best for short

residence time problems.

For another case, consider the previous example, but at some distance downstream add a dilution jet. For this example, the NO<sub>x</sub> post-processor would show the correct evolution of the NO<sub>x</sub> level until the dilution jet. After the dilution jet the post-processor would predict a sudden drop in the NO<sub>x</sub> concentration, due to the sudden change in composition. However what one would expect to happen would be a gradual change in the NO<sub>x</sub> levels, due to the slow NO<sub>x</sub> reaction rates. From this example, it can be concluded that the post processor can be expected to fail when there is sudden changes in the composition of the mixture, except at the initial conditions.

## **Conclusions**

A very fast and reasonably accurate technique has been developed to post-process CFD combustion results and obtain an estimate of the NO<sub>x</sub> levels throughout the field. The method offers a significant improvement over iterative methods in CPU time required, while providing a better prediction than equilibrium techniques. However the method is restricted to cases which have relatively short residence times, and that do not exhibit abrupt changes in composition or temperature.

For the three test cases considered in this paper, the hydrogen-air and methane-air examples showed good agreement with available data. The JetA example did not perform as well, but the deficiencies can be blamed on the poor performance of the full mechanism used to create the look-up tables.

Further work will be required to validate this method, as well as the development of better full mechanisms for JetA-air reaction.

## References

1. U. A. Maas and S. B. Pope. Simplifying chemical kinetics: Intrinsic low-dimensional manifolds in composition space. *Combustion and Flame*, **88**(3/4):239–264, 1992.
2. U. Maas and S. B. Pope. Laminar flame calculations using simplified chemical kinetics based on intrinsic low-dimensional manifolds. In *Twenty-Fifth Symposium (International) on Combustion*, page In Press, 1994.
3. A. T. Norris. Automated simplification of full chemical mechanisms  
. In *33rd AIAA/ASME/SAE/ASEE Joint Propulsion Conference, Seattle, Washington*, 1997. AIAA-97-3115.
4. S. B. Pope and U. Maas. Simplifying chemical kinetics: Trajectory-generated low-dimensional manifolds. Technical Report FDA-93-11, Sibley School of Mechanical and Aerospace Engineering: Fluid dynamics and aerodynamics program, 1993.
5. J. A. Miller and C. T. Bowman. Mechanism and modeling of nitrogen chemistry in combustion. *Prog. Energy Combust. Sci*, **15** :287–338, 1989.
6. R. Kollrack. Model calculations of the combustion product distributions in the primary zone of a gas turbine combustor. In *ASME Winter Annual Meeting, New York NY*, pages ASME 76-WA/GT-7, 1976.

## Acknowledgements

The author would like to thank Dr. A. Brankovic of Pratt and Whitney for providing the test examples for this paper, and for obtaining the JetA-air mechanism. Also thanks are due to Dr. M. Kollatt for providing a simple example to explain the limitations of the method.

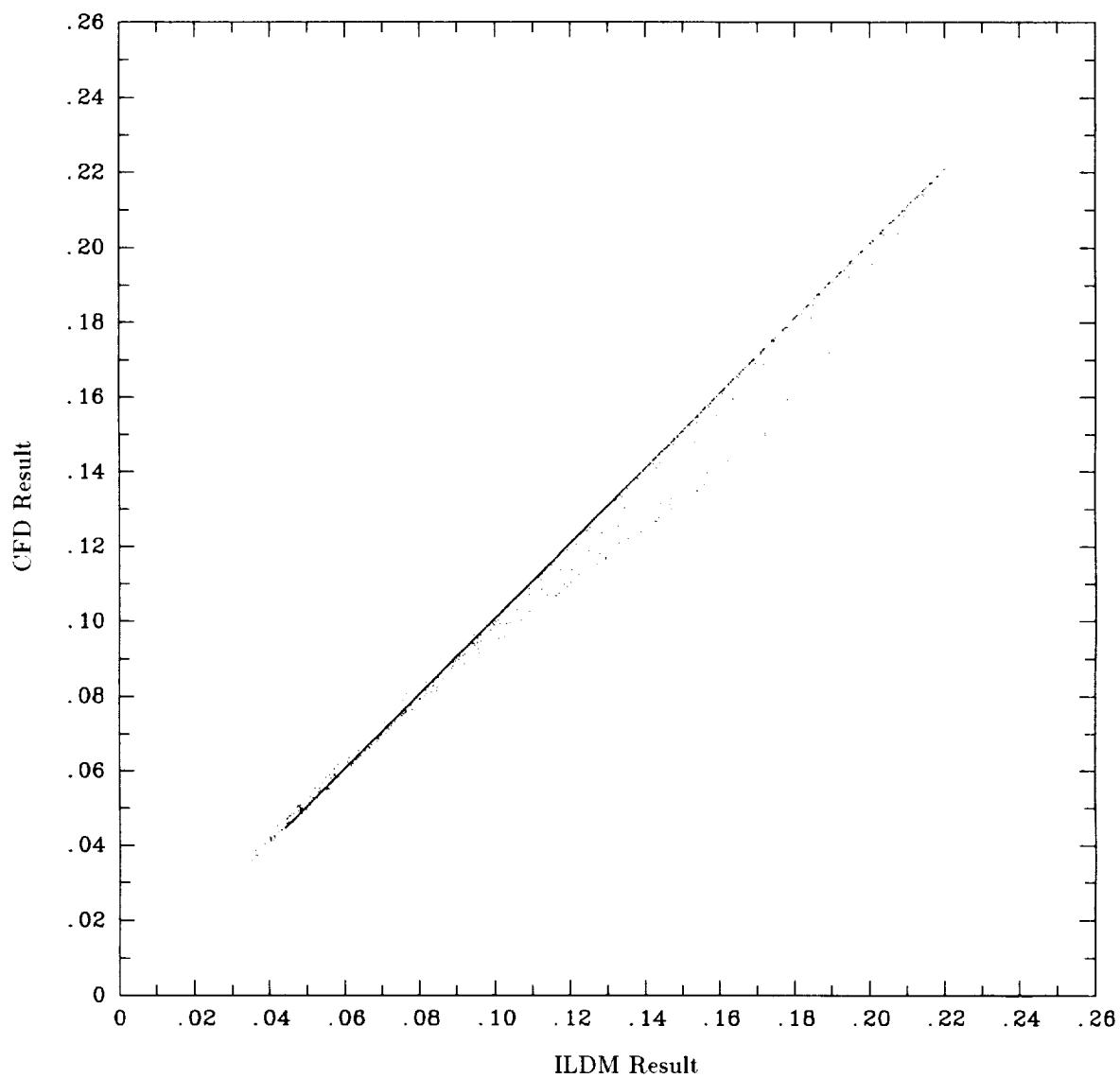


Figure 1: CFD result vs. ILDM prediction for mass fraction of H<sub>2</sub>O in H<sub>2</sub>-air combustor. Mixture fraction range 0.005 to 0.05. Approximately 4,200 samples.



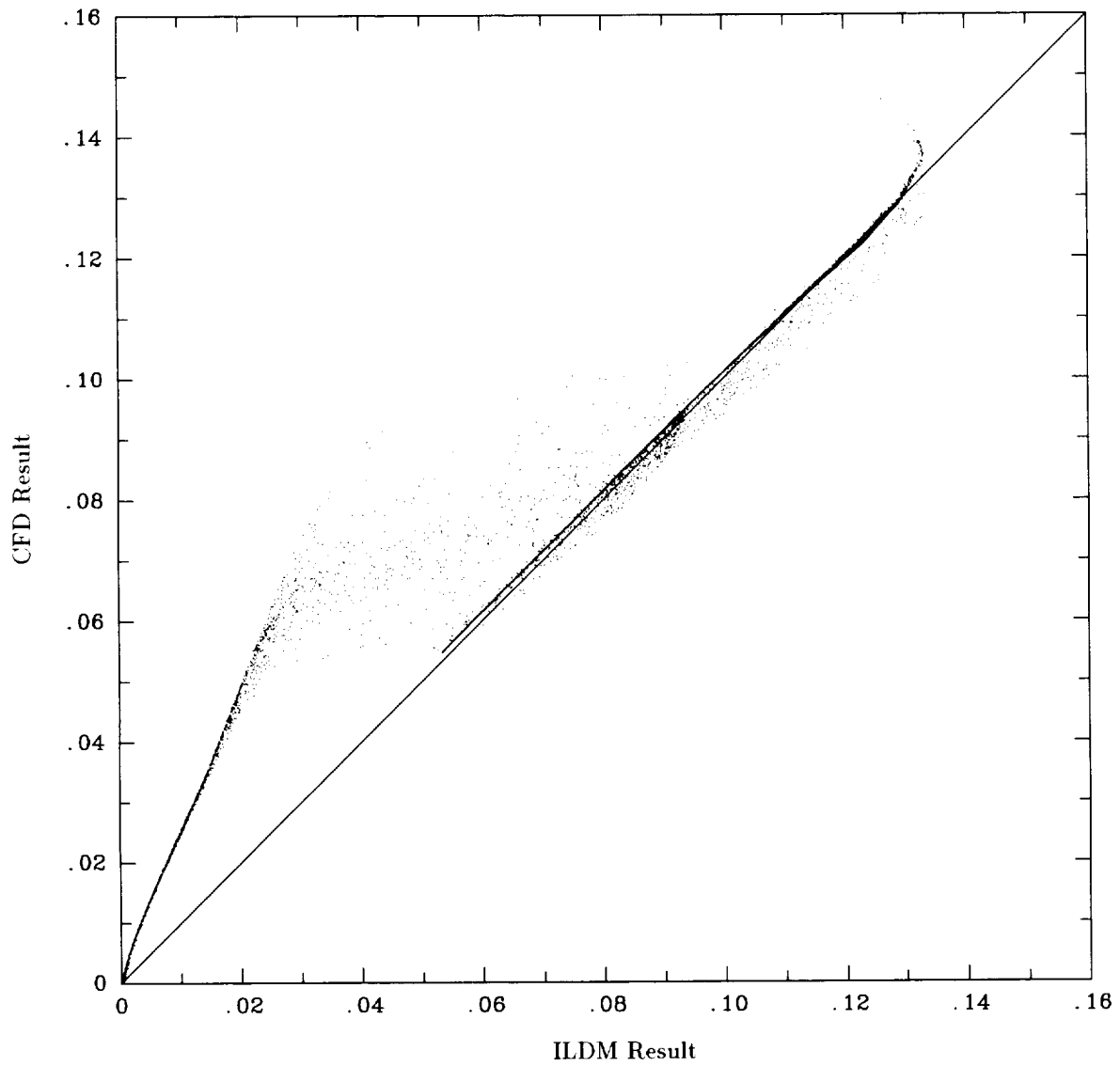


Figure 2: CFD result vs. ILDM prediction for mass fraction of CO<sub>2</sub> in CH<sub>4</sub>-air combustor. Mixture fraction range 0.02 to 0.07. Approximately 10,000 samples.

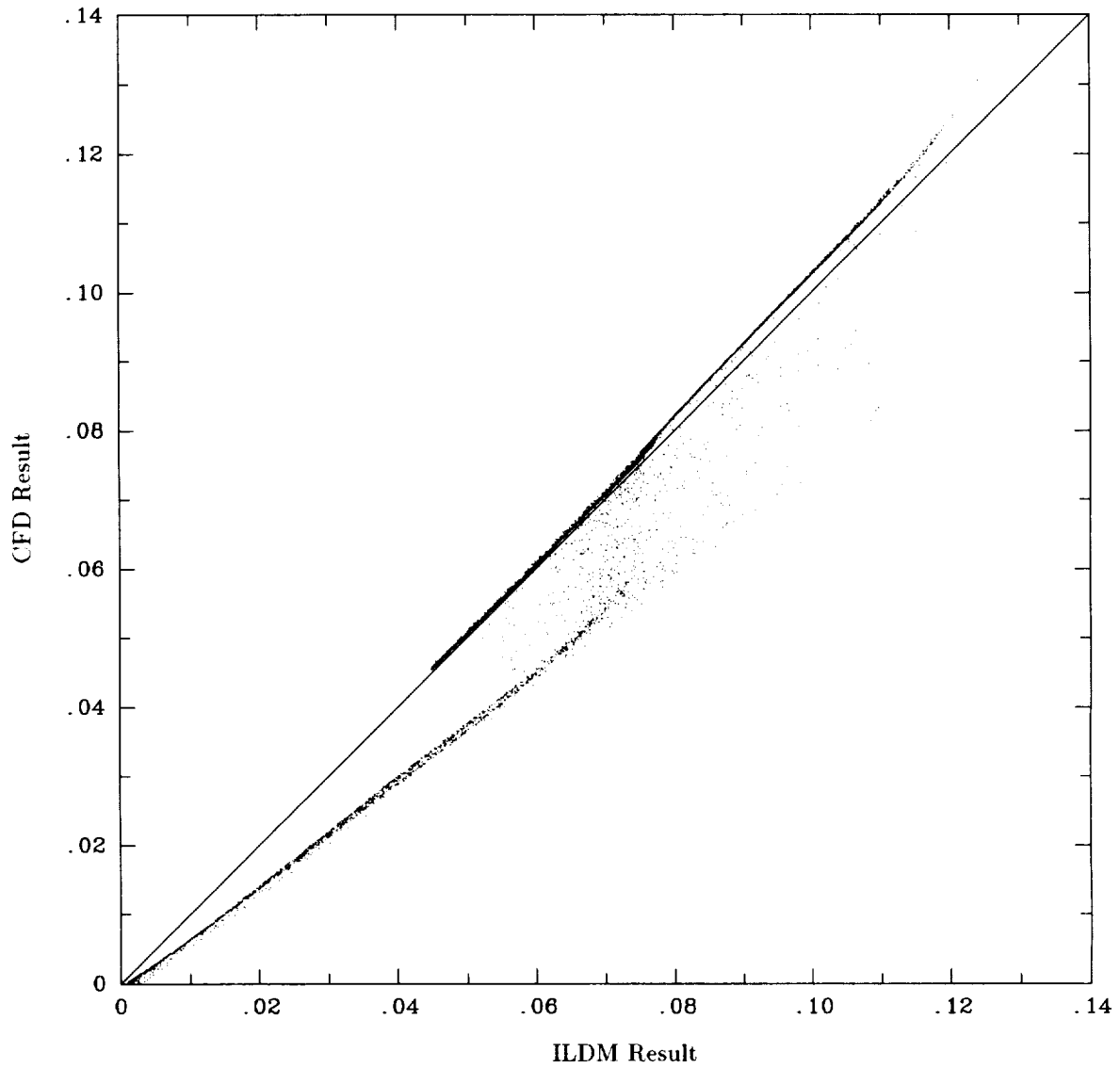


Figure 3: CFD result vs. ILDM prediction for mass fraction of H<sub>2</sub>O in CH<sub>4</sub>-air combustor. Mixture fraction range 0.02 to 0.07. Approximately 10,000 samples.

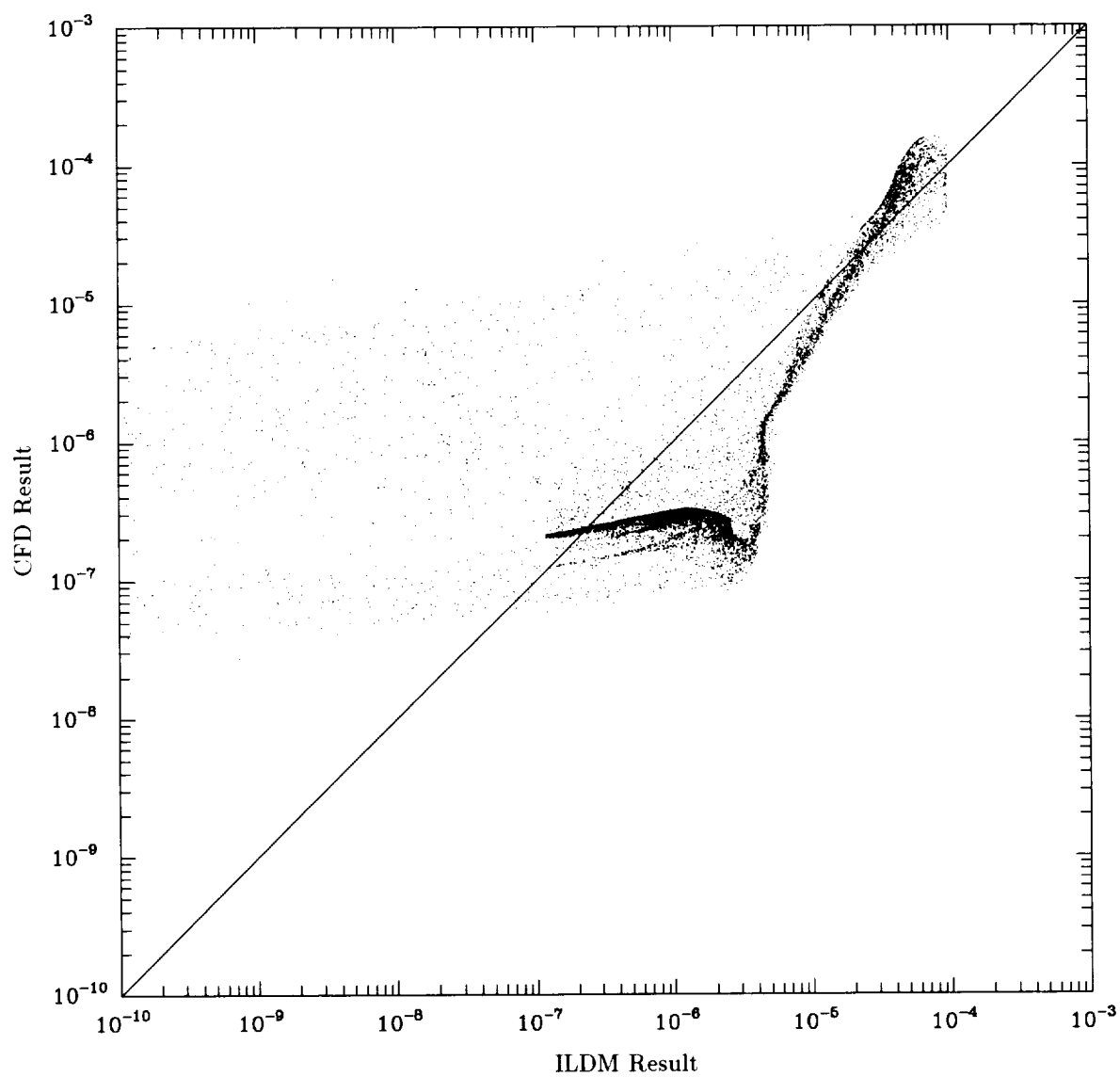


Figure 4: CFD result vs. ILDM prediction for mass fraction of NO in CH<sub>4</sub>-air combustor. Mixture fraction range 0.02 to 0.07. Approximately 10,000 samples.

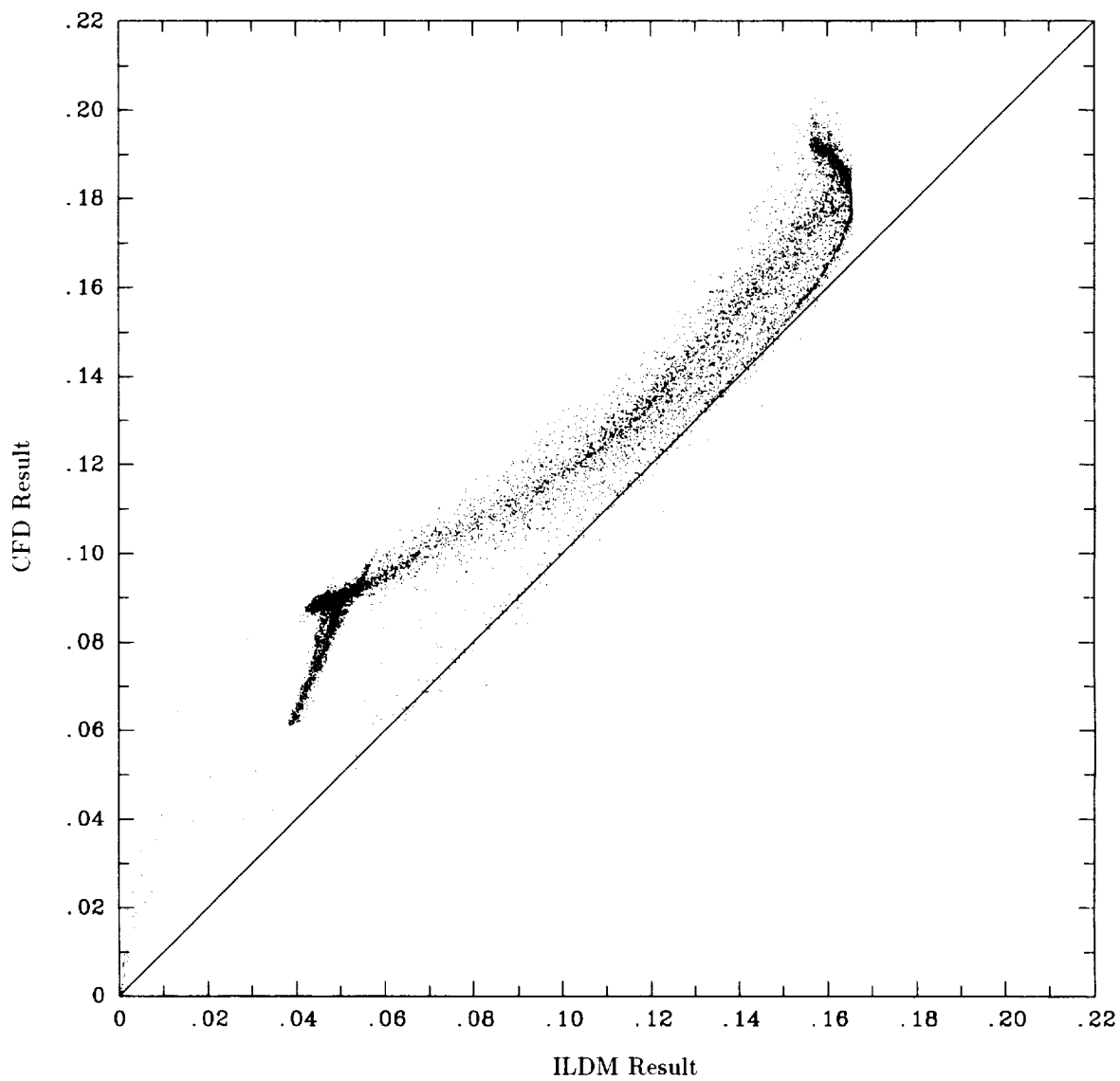


Figure 5: CFD result vs. ILDM prediction for mass fraction of CO<sub>2</sub> in JetA-air combustor. Mixture fraction range 0.02 to 0.07. Approximately 10,000 samples.

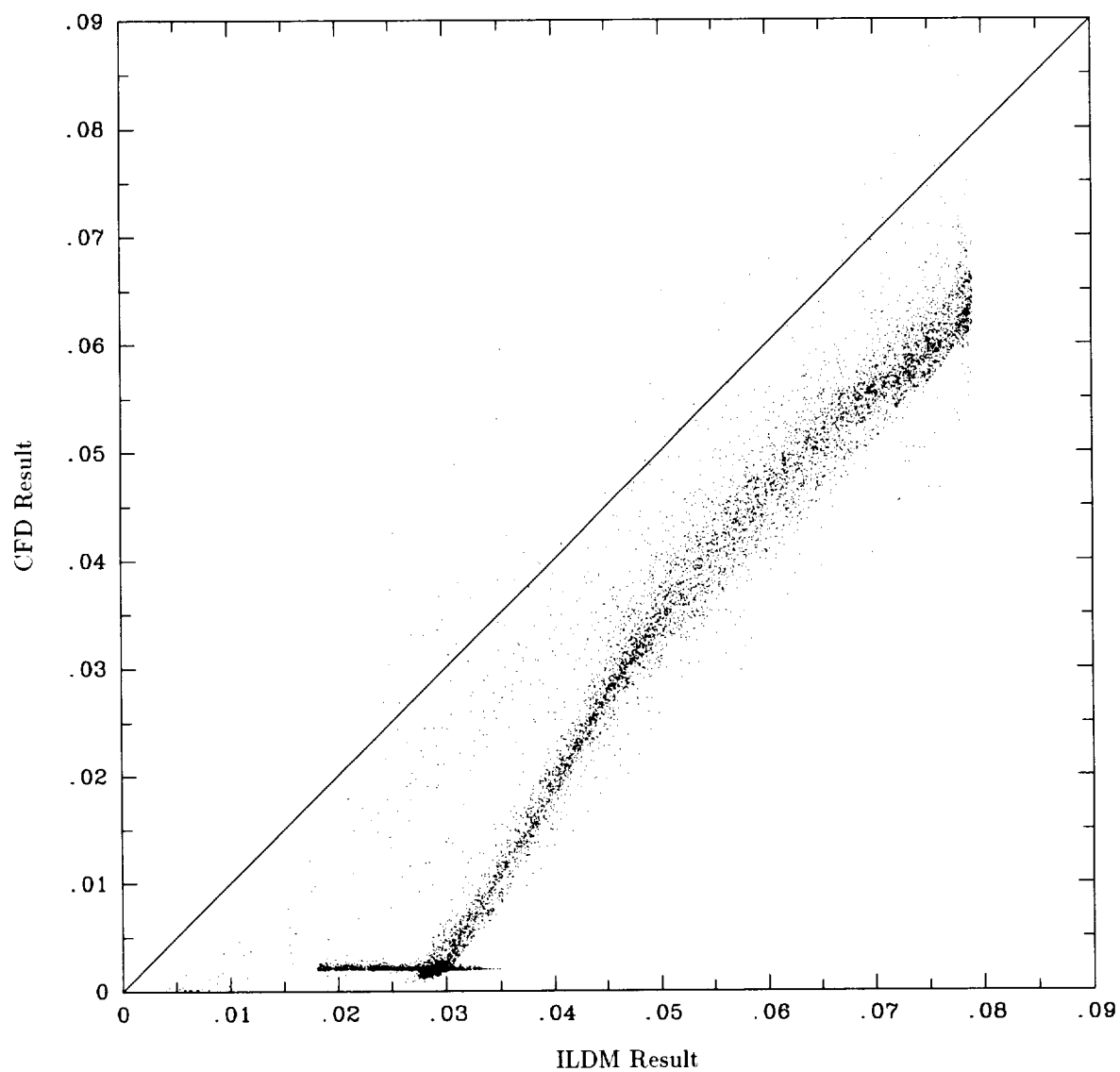


Figure 6: CFD result vs. ILDM prediction for mass fraction of H<sub>2</sub>O in JetA-air combustor. Mixture fraction range 0.02 to 0.07. Approximately 10,000 samples.

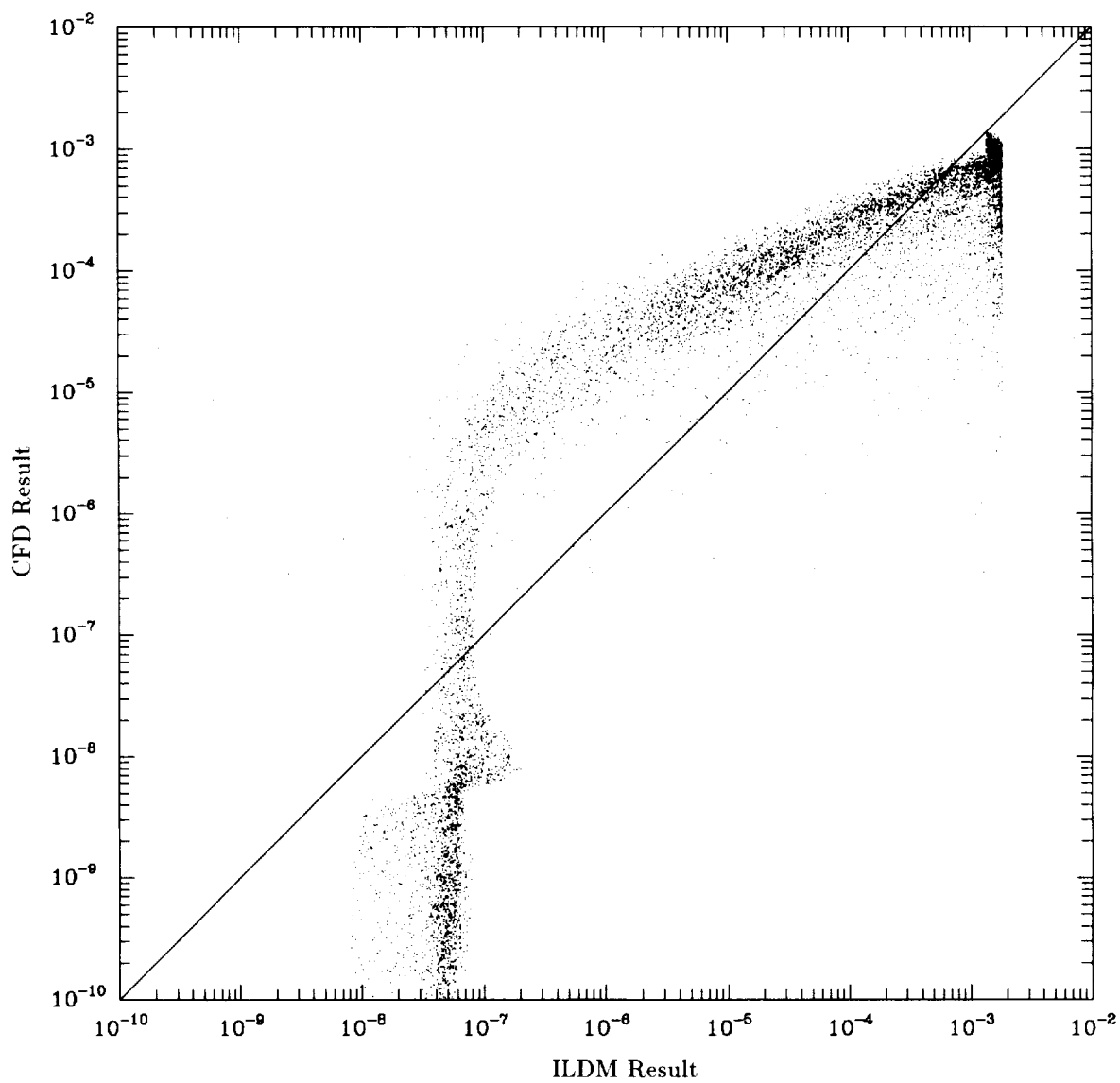


Figure 7: CFD result vs. ILDM prediction for mass fraction of NO in JetA-air combustor. Mixture fraction range 0.02 to 0.07. Approximately 10,000 samples.



REPORT DOCUMENTATION PAGE			Form Approved OMB No. 0704-0188	
Public reporting burden for this collection of information is estimated to average 1 hour per response, including the time for reviewing instructions, searching existing data sources, gathering and maintaining the data needed, and completing and reviewing the collection of information. Send comments regarding this burden estimate or any other aspect of this collection of information, including suggestions for reducing this burden, to Washington Headquarters Services, Directorate for Information Operations and Reports, 1215 Jefferson Davis Highway, Suite 1204, Arlington, VA 22202-4302, and to the Office of Management and Budget, Paperwork Reduction Project (0704-0188), Washington, DC 20503.				
1. AGENCY USE ONLY (Leave blank)		2. REPORT DATE August 1997		3. REPORT TYPE AND DATES COVERED Contractor Report
4. TITLE AND SUBTITLE  Application of Low Dimensional Manifolds in NOx Prediction			5. FUNDING NUMBERS  WU-523-26-33-00 NCC3-534	
6. AUTHOR(S)  A.T. Norris				
7. PERFORMING ORGANIZATION NAME(S) AND ADDRESS(ES)  Institute for Computational Mechanics in Propulsion 22800 Cedar Point Road Cleveland, Ohio 44142			8. PERFORMING ORGANIZATION REPORT NUMBER  E-10854	
9. SPONSORING/MONITORING AGENCY NAME(S) AND ADDRESS(ES)  National Aeronautics and Space Administration Lewis Research Center Cleveland, Ohio 44135-3191			10. SPONSORING/MONITORING AGENCY REPORT NUMBER  NASA CR-204137 ICOMP-97-06; CMOTT-97-01 AIAA-97-3243	
11. SUPPLEMENTARY NOTES  ICOMP Program Director, Louis A. Povinelli, organization code 5800, (216) 433-5818.				
12a. DISTRIBUTION/AVAILABILITY STATEMENT  Unclassified - Unlimited Subject Category 34  This publication is available from the NASA Center for AeroSpace Information, (301) 621-0390.			12b. DISTRIBUTION CODE	
13. ABSTRACT (Maximum 200 words)  A new post-processing technique has been developed, based on the Intrinsic Low Dimensional Manifold (ILDM) method of Maas and Pope. The ILDM method is a dynamical systems approach to the simplification of large chemical kinetic mechanisms. By identifying low-dimensional attracting manifolds, the method allows complex full mechanisms to be parameterized by just a few variables: In effect, generating reduced chemical mechanisms by an automatic procedure. These resulting mechanisms however, still retain all the species used in the full mechanism. The NOx post-processor takes an ILDM reduced mechanism and attempts to map this mechanism to the results of a CFD calculation. This mapping allows the NOx concentrations at each grid node to be obtained from the ILDM reduced mechanism, as well as other trace species of interest. Because a mapping procedure is used, this method is very fast, being able to process one million node calculations in just a few minutes.				
14. SUBJECT TERMS  NOx; Pollutant prediction; Manifold methods; Post-processing			15. NUMBER OF PAGES 13	
			16. PRICE CODE A03	
17. SECURITY CLASSIFICATION OF REPORT Unclassified	18. SECURITY CLASSIFICATION OF THIS PAGE Unclassified	19. SECURITY CLASSIFICATION OF ABSTRACT Unclassified	20. LIMITATION OF ABSTRACT	